

AD-A210 498

T DOCUMENTATION PAGE

Form Approved
OMB No. 0704-0188

1b. RESTRICTIVE MARKINGS

3. DISTRIBUTION/AVAILABILITY OF REPORT

Approved for public release ;
Distribution unlimited

2b. DECLASSIFICATION/DOWNGRADING SCHEDULE

4. PERFORMING ORGANIZATION REPORT NUMBER(S)

5. MONITORING ORGANIZATION REPORT NUMBER(S)

EOARD-TR-89-10

6a. NAME OF PERFORMING ORGANIZATION

C.N.R.S. - LABORATOIRE DE PHY-
SIQUE MOLECULAIRE & ATMOSPHERIQUE6b. OFFICE SYMBOL
(if applicable)

7a. NAME OF MONITORING ORGANIZATION

European Office of Aerospace Research and
Development

6c. ADDRESS (City, State, and ZIP Code)

Tour 13, Université P. & M. Curie
4, Place Jussieu
75252 PARIS CEDEX 05

7b. ADDRESS (City, State, and ZIP Code)

223/231 Old Marylebone Rd
London NW1 5TH UK8a. NAME OF FUNDING/SPONSORING
ORGANIZATIONEuropean Office of Aerospace
Research & Development8b. OFFICE SYMBOL
(if applicable)

LDG

9. PROCUREMENT INSTRUMENT IDENTIFICATION NUMBER

AFOSR 87-0296

8c. ADDRESS (City, State, and ZIP Code)

223/231 Old Marylebone Rd
LONDON NW1 5TH UK

10. SOURCE OF FUNDING NUMBERS

PROGRAM
ELEMENT NO.
61102FPROJECT
NO.
2301TASK
NO.
D1WORK UNIT
ACCESSION NO.
008

11. TITLE (Include Security Classification)

INTENSITY MEASUREMENTS OF INFRARED CARBON DIOXIDE BANDS

12. PERSONAL AUTHOR(S)

V. DANA

13a. TYPE OF REPORT

FINAL

13b. TIME COVERED

FROM JUL 87 TO JUL 88

14. DATE OF REPORT (Year, Month, Day)

1988/July/14

15. PAGE COUNT

16. SUPPLEMENTARY NOTATION

17. COSATI CODES

FIELD	GROUP	SUB-GROUP

18. SUBJECT TERMS (Continue on reverse if necessary and identify by block number)

Infrared, Intensities, Broadening coefficients,
Carbon Dioxide

19. ABSTRACT (Continue on reverse if necessary and identify by block number)

This report summarizes the results of intensities and broadening coefficients measurements performed on $^{12}\text{C}^{16}\text{O}_2$ lines in the $13.5\mu\text{m}$ region. The used spectra were recorded at high resolution with a Fourier transform spectrometer.

From the intensities measurements it has been possible to derive the variation of the square of the transition dipole moment $(\mu)^2$ with respect to the rotational quantum numbers.

20. DISTRIBUTION/AVAILABILITY OF ABSTRACT

☒ UNCLASSIFIED/UNLIMITED ☐ SAME AS RPT. ☐ DTIC USERS

21. ABSTRACT SECURITY CLASSIFICATION

Unclassified

22a. NAME OF RESPONSIBLE INDIVIDUAL

OWEN R. COTE

22b. TELEPHONE (Include Area Code)

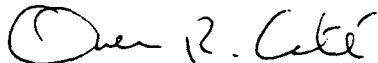
(44 1) 409-4437

22c. OFFICE SYMBOL

LDG

This report has been reviewed by the EOARD Information Office and is releasable to the National Technical Information Service (NTIS). At NTIS it will be releasable to the general public, including foreign nations.

This technical report has been reviewed and is approved for publication.



OWEN R. COTE'
Chief, Geophysics and Space



FRED T. GILLIAM, Lt. Col, USAF
Chief Scientist

SCIENTIFIC REPORT

Grant number : AFOSR-87-0296

INTENSITY MEASUREMENTS OF INFRARED CARBON DIOXIDE BANDS

Victor Dana

Labcratoire de Physique Moléculaire et Atmosphérique
Tour 13 - Université Pierre et Marie Curie et CNRS
4, Place Jussieu - 75252 Paris Cedex 05, France



Accession For	
NTIS GRA&I	<input checked="" type="checkbox"/>
DTIC TAB	<input type="checkbox"/>
Unannounced	<input type="checkbox"/>
Justification	
By	
Distribution	
Availability Codes	
Dist	
A-1	

Prepared for : European Office of Aerospace Research en Development
223/231 Old Marylebone Road, London NW1 5TH, UK

I - INTRODUCTION

CO_2 is an atmospheric gas which plays an important role in the atmosphere and is often measured by remote sensing in the $13.5 \mu\text{m}$ region. So it is necessary in order to perform reliable analysis of the atmospheric spectra to have accurate data on the positions, intensities and broadening coefficients of the lines arising in this region. The line positions are well known but some uncertainties remain on the intensities and broadening coefficients. The goal of this work is to improve these parameters for CO_2 lines in the region of $13.5 \mu\text{m}$. For that, we have developed in the present work a method which allows an accurate derivation of intensities and broadening coefficients from interferometer spectra. The performances of this method were checked in a preliminar work by studying the $11101 \leftarrow 10002$ band of $^{12}\text{C}^{16}\text{O}_2$ [1]. Then, we have measured lines intensities of the following bands :

11101 \leftarrow 10002	centered at 791.447 cm^{-1}	[2]
11101 \leftarrow 02201	centered at 741.724 cm^{-1}	
10001 \leftarrow 01101	centered at 720.805 cm^{-1}	
20002 \leftarrow 10002	centered at 738.673 cm^{-1}	[3]
12201 \leftarrow 03301	centered at 757.479 cm^{-1}	[3]

Besides, for each band we have deduced from the line intensities the square of the transition dipole moment and Herman Wallis coefficients.

In addition we have measured for lines belonging to the $11101 \leftarrow 10002$ band the self, N_2 - and O_2 -broadening coefficients.

II - DESCRIPTION OF THE METHOD*

This method allows to derive simultaneously the intensity and the width of an isolated line through the adjustment of a calculated line shape to the experimental one.

The calculated line shape $G(\sigma)$ is obtained by convolving the true line shape $G_t(\sigma)$ with the response function F of the interferometer.

$G_t(\sigma)$ is given by the well known expression

$$G_t(\sigma) = I_0(\sigma) \exp[-K(\sigma, P)\ell]$$

* This method is extensively described in Ref.[1]

where $K(\sigma, P)$ is the absorption coefficient ; it depends on the intensity and on the line width. $K(\sigma, P)$ is well described by a Voigt profile. P is the gas pressure, ℓ is the path length in the absorbing gas. $I_0(\sigma)$ is the beam intensity in absence of absorption.

The response function F of an interferometer is the Fourier transform of the filtering function $\mathcal{A}(D)$. Usually the filtering function used to calculate the response function is a "boxcar" ; in this work we have chosen a filtering function which decreases in a parabolic way with the path difference D , in order to take into account the influence of the entrance iris of the interferometer (see Fig.1).

Finally for each line we compute a succession of values of the transmitted intensity $I_t(n)$ separated by a constant interval $d\sigma$ in wavenumber unit. The value of $d\sigma$ is chosen equal to the interval separating two experimental data.

The best adjustment of the calculated line shape to the experimental one is obtained when the two following quantities are minimized simultaneously :

1. The quadratic differences ΔI

$$\Delta I = \sum_n (I_{t \text{ exp}} - I_{t \text{ calc}})^2$$

2. The differences between the areas of experimental and calculated line shape.

III - CHARACTERISTICS OF THE FOURIER TRANSFORM SPECTROMETER

The step by step Fourier transform spectrometer used in our work was built in our laboratory by L. Henry, A. Valentin and Ch. Nicolas.

The path difference of this interferometer can reach 22 meters which gives an apparatus function width of $5 \times 10^{-4} \text{ cm}^{-1}$. This unevacuated interferometer covers the spectral range 3-19 μm within the atmospheric windows. The signal to noise ratio is about 200 around 10 μm using a mercury or copper doped germanium detector and 500 at 5 μm with an indium antimonide detector. The absolute precision on the wavenumbers measurements is better than $2 \times 10^{-4} \text{ cm}^{-1}$.

IV - SPECTRA ANALYSIS

The different spectra used in this work were recorded with a GeHg or GeCu detector with a cooled low pass interference filter. On these spectra the signal to noise ratio is close to 200. The gas pressure inside the cell was measured with an relative uncertainty better than 1%. The temperature was measured on the walls of the cell and we assume that a thermal equilibrium between the gas sample

and the cell was established. The gas sample was 99.998% minimum purity CO_2 purchased from Air Liquide.

One of the most difficult problem we had to solve was the elimination of fringes which arise from reflections on the opposite side of the beam splitter. For that we have used two procedures :

1. Empty cell spectra were recorded before and after the spectrum of the gas sample in order to eliminate these fringes by ratioing but it seems that this procedure introduces a systematic error of a few percents (4-6%) on the intensities values.

2. In the second method, for each line we determine by an adjustment the local fringes pattern which is then eliminated numerically. This method increases the internal coherence between the results obtained from different recorded spectra.

V - LINES INTENSITY

The line intensity $S(J)$ is given by

$$S(J) = \frac{8\pi^3}{3hc} \cdot \frac{N_T \cdot I_a}{Q(T)} \sigma(J) \left[1 - \exp\left(-\frac{hc}{kT} \sigma(J)\right) \right] \exp\left(-\frac{hc}{kT} E(v,J)\right) \cdot (\mu)^2 \cdot L(J)$$

where N_T is the total number of molecules per cm^3

$Q(T)$ is the total internal partition function

I_a is the isotopic abundance ($I_a = 0.985$)

$\sigma(J)$ is the wavenumber of the transition (in cm^{-1})

$E(v,J)$ is the lower state energy of the transition (in cm^{-1})

$(\mu)^2$ is the square of the transition dipole moment

$L(J)$ is the Hönl-London factor.

Using this expression the $(\mu)^2$ values are deduced from the measured lines intensities. Assuming that the variation of $(\mu)^2$ with respect to the rotational quantum numbers is described by the following expansions

$$\begin{aligned} (\mu)^2 &= (\mu_0)^2 \left\{ 1 + 2A_1 m + 2A_2 J'(J'+1) \right\} && \text{in P and R branches} \\ \text{and } (\mu)^2 &= (\mu_0)^2 \left\{ 1 + 2A_3 J(J+1) \right\} && \text{in the Q branch} \end{aligned}$$

We have, through a least squares procedure, derived for each band, the values of $(\mu_0)^2$, A_1 , A_2 and A_3 . It is important to remark that it is difficult to determine accurately the A_2 coefficient because the effect of the quadratic term $A_2 J'(J'+1)$ is very weak.

VI - RESULTS

1) Intensities

On the Tables concerning the lines intensities are listed the measured values. In addition are given, on these tables, the intensities calculated by using the values of $(\mu_0)^2$, A_1 , A_2 and A_3 . In the last column are given the differences in percent.

On Table VI are given for each band the values of $(\mu_0)^2$, A_1 , A_2 and A_3 .

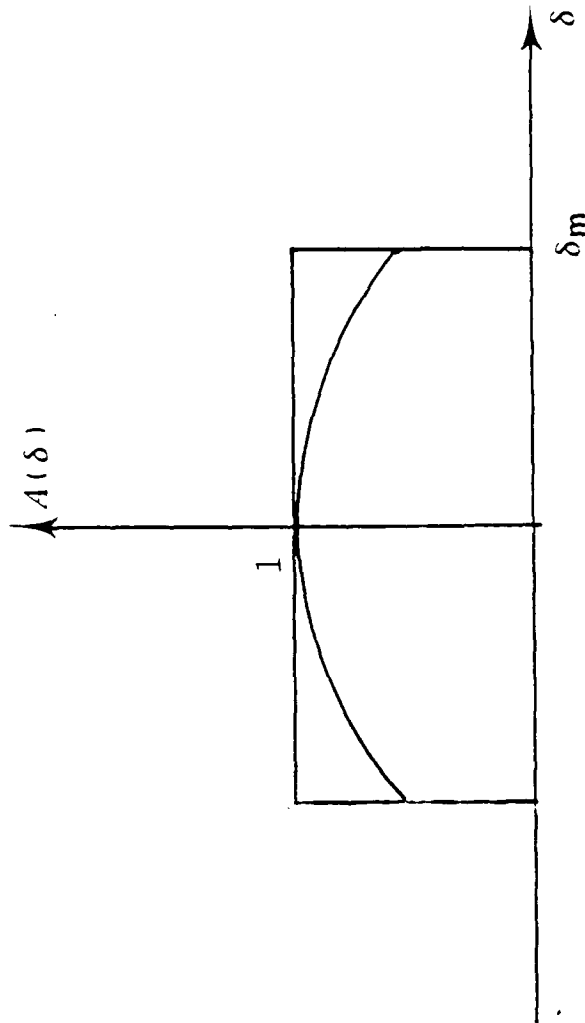
2) Broadening parameters

On Tables VII, VIII and IX are listed the values of self-, N_2 - and O_2 -broadening coefficients of lines belonging to the 11101 \leftarrow 10002 band of $^{12}C^{16}O_2$; results proposed by other authors are given.

R E F E R E N C E S

- [1] V. Dana and A. Valentin
Determination of line parameters from FTS spectra.
Appl. Optics 27(21), 4450-4453 (1988).
- [2] V. Dana, A. Valentin, A. Hamdouni and L.S. Rothman
Line intensities and broadening parameters of the 11101 \leftarrow 10002 band of $^{12}\text{C}^{16}\text{O}_2$.
Appl. Optics (in press)
- [3] A. Valentin, V. Dana and A. Hamdouni
Absolute intensities of lines in the 20002 \leftarrow 11102 and 12201 \leftarrow 03301 bands of $^{12}\text{C}^{16}\text{O}_2$.
(to be published)

THE APPARATUS FUNCTION IS THE FOURIER TRANSFORM OF THE $A(\delta)$ FUNCTION



$$\left\{ \begin{array}{l} A(\delta) = 1 \\ A(\delta) = 0 \end{array} \right. \begin{array}{l} -\delta_m < \delta < \delta_m \\ \delta < -\delta_m \text{ AND } \delta > \delta_m \end{array} \Rightarrow \text{THE APPARATUS FUNCTION IS } \frac{\sin x}{x}$$

WHEN THE EFFECT OF THE ENTRANCE DIAPHRAGM OF THE INTERFEROMETER IS TAKEN INTO ACCOUNT, THE $A(\delta)$ FUNCTION HAS A PARABOLIC SHAPE : THE FOURIER TRANSFORM OF $A(\delta)$ GIVES THE REAL APPARATUS FUNCTION.

Table I

Line	Measured ^(a) intensities (cm/mol×10 ²³)	Calculated intensities (cm/mol×10 ²³)	$\frac{O - C}{O}$ (in %)
P26	0.839	0.844	-0.6
P24	0.982	0.951	+3.1
P22	1.055	1.048	+0.6
P18	1.156	1.180	-2.1
P16	1.166	1.199	-2.8
P14	1.160	1.178	-1.6
P12	1.109	1.114	-0.5
P10	1.016	1.002	+1.4
P 8	0.854	0.844	+1.1
P 6	0.638	0.642	-0.6
Q18	2.722	2.681	+1.5
Q20	2.514	2.548	-1.3
Q22	2.434	2.362	+3.0
Q24	2.163	2.136	+1.2
Q26	1.863	1.892	-1.5
Q28	1.649	1.637	+0.7
Q30	1.377	1.388	-0.8
Q32	1.148	1.155	-0.6
Q34	- 0.956	0.940	+1.6
Q36	0.739	0.753	-1.9
R 4	0.842	0.832	+1.2
R 6	1.056	1.069	-1.3
R 8	1.293	1.270	+1.8
R10	1.427	1.424	+0.2
R12	1.542	1.528	+0.9
R14	1.573	1.584	-0.7
R16	1.556	1.591	-2.3
R18	1.519	1.553	-2.2
R20	1.470	1.480	-0.7
R22	1.373	1.375	-0.1
R24	1.225	1.249	-2.0
R26	1.139	1.111	+2.4
R28	1.004	0.969	+3.5
R30	0.844	0.828	+1.9
R32	0.680	0.694	-2.1
R34	0.564	0.572	-1.3

(a) In natural abundance.

Line intensities for the 11101 + 10002 band of $^{12}\text{C}^{16}\text{O}_2$

Table II

Line	$\sigma(J)$ (cm^{-1})	Obs ($10^{23} \text{ cm}^{-1} /$ molecule cm^{-2})	Calc	Obs - Calc Obs (in per cent)
P31	713.3775	0.2044	0.2084	-2.0
P21	721.7730	0.3924	0.3978	-1.4
P17	725.0702	0.4644	0.4407	+5.1
Q24	737.4041	0.7892	0.7529	+4.6
Q26	737.1900	0.6674	0.6770	-1.4
Q30	736.7128	0.5320	0.5177	+2.7
Q38	735.5673	0.2360	0.2428	-2.9
R 5	743.3123	0.2014	0.2157	-7.1
R11	747.8656	0.3949	0.3953	-0.1
R13	749.3647	0.4183	0.4267	-2.0
R15	750.8538	0.4620	0.4421	+4.3
R17	752.3335	0.4230	0.4442	-5.0
R25	758.1583	0.3535	0.3455	+2.3
R27	759.5908	0.3143	0.3072	+2.3
R33	763.8339	0.1875	0.1896	-1.1

Line intensities for the 20002 + 11102 band of $^{12}\text{C}^{16}\text{O}_2$

Table III

Line	$\sigma(J)$ (cm^{-1})	Obs ($10^{+23} \text{ cm}^{-1} /$ molecule cm^{-2})	Calc	$\frac{\text{Obs} - \text{Calc}}{\text{Obs}}$ (in per cent)
P18	743.1033	0.2660	0.2541	+4.4
P15	745.5351	0.2852	0.2725	+4.4
P11	748.7559	0.2642	0.2744	-3.9
P 9	750.3567	0.2561	0.2660	-3.9
P 8	751.1550	0.2499	0.2590	-3.6
P 7	751.9508	0.2442	0.2505	-2.6
P 5	753.5384	0.2370	0.2309	+2.6
Q25	756.9438	0.3333	0.3308	+0.7
Q26	756.8944	0.3089	0.3121	-1.0
Q27	756.8574	0.2831	0.2932	-3.6
Q28	756.8029	0.2702	0.2735	-1.2
Q31	756.6663	0.2228	0.2162	+3.0
Q32	756.5990	0.1983	0.1980	-0.1
Q33	756.5618	0.1814	0.1804	+0.5
R14	769.0495	0.1687	0.1622	+3.8
R15	769.8066	0.1719	0.1698	+1.2
R16	770.5639	0.1759	0.1724	+2.0
R17	771.3168	0.1678	0.1749	-4.2

Line intensities for the 12201 + 03301 band of $^{12}\text{C}^{16}\text{O}_2$

TABLE IV

J	Obs (10^{22} cm $^{-1}$ / molecule cm $^{-2}$)	Calc	Obs - Calc
			Obs (in per cent)
P25	4.480	4.316	+ 3.7
P24	4.433	4.588	- 3.5
P23	4.758	4.862	- 2.2
P19	5.530	5.789	- 4.7
P17	5.840	6.104	- 4.5
P15	6.306	6.275	+ 0.5
P13	6.219	6.276	- 0.9
P12	6.372	6.215	+ 2.5
P11	6.573	6.103	+ 7.2
P8	5.742	5.471	+ 4.7
Q33	4.793	4.747	+ 1.0
Q25	8.656	8.679	- 0.3
R5	1.868	1.832	+ 1.9
R6	2.312	2.309	+ 0.1
R7	2.827	2.762	+ 2.3
R8	3.204	3.185	+ 0.6
R9	3.685	3.572	+ 3.1
R10	4.168	3.915	+ 6.1
R11	4.409	4.222	+ 4.2
R12	4.248	4.479	- 5.4
R13	4.492	4.690	- 4.4
R14	5.050	4.858	+ 3.8
R15	4.644	4.976	- 7.1
R16	4.817	5.049	- 4.5
R17	4.720	5.085	- 7.7
R18	5.009	5.070	- 1.2
R20	4.964	4.941	+ 0.5
R22	4.666	4.681	- 0.3
R24	4.172	4.325	- 3.7
R25	4.035	4.119	- 2.1
R29	3.144	3.220	- 2.5
R33	2.255	2.315	- 2.7
R34	2.217	2.100	+ 5.3
R35	1.835	1.905	- 3.8
R36	1.719	1.713	+ 0.3
R37	1.502	1.538	- 2.4
R38	1.368	1.370	- 0.1
R39	1.235	1.219	+ 1.3
R40	1.094	1.077	+ 1.6
R41	.9430	.950	- 0.7
R42	.8693	.8307	+ 4.4
R43	.6742	.7264	- 7.7
R44	.6501	.6297	+ 3.1
R46	.4899	.4691	+ 4.2
R47	.4163	.4035	+ 3.1

Line intensities for the 11101 + 02201 band of $^{12}\text{C}^{16}\text{O}_2$.

TABLE V

J	Obs (10^{21} cm $^{-1}$ / molecule cm $^{-2}$)	Calc	Obs - Calc
			Obs (in per cent)
R63	.1098	.1035	+ 5.7
R61	.1593	.1600	- 4.4
R55	.5352	.5349	+ 0.0
R51	1.026	1.102	- 7.4
R 3	8.656	8.276	+ 4.4
R 1	2.700	2.794	- 3.5
Q48	3.202	3.146	+ 1.7
Q46	4.649	4.956	- 6.6
Q44	6.326	5.831	+ 7.8
Q42	7.843	7.741	+ 1.3
Q40	9.490	10.105	- 6.5
P37	6.447	6.398	+ 0.7

Line intensities for the 10001 + 01101 band of $^{12}\text{C}^{16}\text{O}_2$

TABLE VI

BAND	$(\mu_0)^2$	A_1	A_2	A_3
11101 \leftarrow 10002	$1.323 \cdot 10^{-3} \pm 7.1 \cdot 10^{-6}$	$1.0 \cdot 10^{-3} \pm 1.1 \cdot 10^{-4}$	$-1.6 \cdot 10^{-3} \pm 6 \cdot 10^{-6}$	$-3.5 \cdot 10^{-3} \pm 4.5 \cdot 10^{-6}$
20002 \leftarrow 11102	$1.055 \cdot 10^{-2} \pm 1.3 \cdot 10^{-4}$	$3.44 \cdot 10^{-4} \pm 2.9 \cdot 10^{-4}$		$5.12 \cdot 10^{-3} \pm 1.2 \cdot 10^{-6}$
12201 \leftarrow 03301	$1.422 \cdot 10^{-2} \pm 1.4 \cdot 10^{-4}$	$1.07 \cdot 10^{-3} \pm 3.6 \cdot 10^{-4}$		$1.33 \cdot 10^{-3} \pm 8.6 \cdot 10^{-6}$
11101 \leftarrow 02201	$1.456 \cdot 10^{-2} \pm 1.0 \cdot 10^{-4}$	$9.01 \pm 1.3 \cdot 10^{-4}$		$2.35 \cdot 10^{-3} \pm 4.3 \cdot 10^{-6}$
10001 \leftarrow 01101	$1.425 \cdot 10^{-2} \pm 3.9 \cdot 10^{-4}$	$1.17 \pm 3.0 \cdot 10^{-4}$		

Transition moment constants $(\mu_0)^2$, A_1 , A_2 and A_3 for the studied CO₂ Bands.

Table VII

$ m $	Present work 11101 \leftarrow 10002 T=294.5 K	Ref [5] 01111 \leftarrow 01101 T=300 K	Ref [6] (a) T=296 K
8	0.1050	0.1152	0.1104
10	0.1040	0.1078	0.1080
12	0.1010	0.1057	0.1054
13	0.1025	0.1026	0.1042
14	0.0993	0.1035	0.1031
15	0.1015	0.1041	0.1020
16	0.0973	0.1014	0.1010
17	0.0983	0.1003	0.1000
18	0.0963	0.0991	0.0990
21	0.0927	0.0983	0.0962
22	0.0935	0.0973	0.0953
23	0.0926		0.0944
25	0.0910	0.0970	0.0928
27	0.0905	0.0916	0.0910
29	0.0880	0.0893	0.0891
31	0.0865	0.0878	0.0871
33	0.0845	0.0886	0.0851
37	0.0795	0.0838	0.0813
39	0.0780		0.0797
41	0.0760	0.0818	0.0780

(a) : smoothed values from measurements on the 00011 \leftarrow 00001 and the 10011 \leftarrow 10002 bands

Table VIII

$ m $	Present work 11101 \leftarrow 10002 T=294.8 K	Ref [5] 01111 \leftarrow 01101 T=300 K	Ref [6] (a) T=296 K
5	0.0840	0.0860	0.0854
7	0.0820	0.0846	0.0830
8	0.0815	0.0804	
11	0.0790	0.0820	0.0795
12	0.0780	0.0786	
14	0.0765	0.0794	
15	0.0780	0.0773	0.0768
16	0.0725	0.0773	
17	0.0750	0.0765	0.0755
19	0.0740	0.0754	0.0744
21	0.0715	0.0741	0.0735
22	0.0700	0.0732	
23	0.0720	0.0732	0.0726
25	0.0705	0.0735	0.0718
27	0.0695	0.0726	0.0712
31	0.0700	0.0712	0.0701
35	0.0675	0.0694	0.0693
37	0.0670	0.0709	0.0689
39	0.0667	0.0679	0.0687

(a) : smoothed values from measurements on the 00011 \leftarrow 00001 and the 10011 \leftarrow 00001 bands

Table IX

$ m $	Present work 11101 \leftarrow 10002 T=294.8 K	Ref [6] (a) T=296 K
5	0.0730	0.0750
6	0.0742	
8	0.0738	
10	0.0680	
11	0.0685	0.0690
12	0.0660	
13	0.0666	0.0675
14	0.0651	
16	0.0637	
17	0.0640	0.0649
18	0.0617	
19	0.0622	0.0637
20	0.0613	
21	0.0616	0.0626
22	0.0595	
23	0.0606	0.0617
25	0.0577	0.0609
27	0.0565	0.0602

(a) : smoothed values from measurements on the 00011 \leftarrow 00001 and the
10011 \leftarrow 00001 bands